Section 2

ADVANCED TECHNOLOGY DEVELOPMENTS

2.A Laser-Beam Apodizer Utilizing Gradient-Index Optical Effects in Liquid Crystals

Laser-beam apodization has been a goal of solid-state laser programs since the early 1970s. Apodization is the shaping of the spatial beam profile to increase the fill factor through the gain medium. This allows more energy to be extracted and also reduces linear and nonlinear edge-diffraction effects that cause self-focusing spikes. A beam apodizer determines, to a large extent, the ultimate performance of a high-power laser system.

An ideal beam apodizer possesses the following characteristics[1]:
1. The slope of the transmission function should be such that the radial distance between the 90% and 10% transmission points is at least $3\lambda L/d$, where λ is the laser wavelength, L is the propagation distance over which intensity modulation should be minimal, and d is the beam diameter. One of the transmission functions that approximates this condition is a super-Gaussian of order N, that is,

$$T(r) = \exp\left[-(r/r_0)^N\right],\tag{1}$$

where the radial clear aperture r_0 is selected based on the condition that $T(r_1) = 10^{-3}$, where $2r_1$ is the entry aperture of the amplifying device that follows the apodizer.

2. Wave-front quality over the clear aperture and into the soft edge is a smooth function with continuous first derivatives.

29

3. The peak-to-minimum transmission ratio is at least 1000 to 1.

4. High laser-damage threshold at the design wavelength and pulse width.

5. Environmental stability.

Several techniques for apodizing laser beams have been reported.[1-11] Recently, S. D. Jacobs *et al.* have developed a new apodizer based on liquid-crystal technology that has demonstrated properties resembling those of a perfect apodizer.[12] However, their device concept works best for small clear apertures, and the exponential relationship used to model the reflectivity of their cholesteric liquid crystal (CLC) as a function of thickness is valid only as a first approximation.

In this article, we propose a novel beam apodizer utilizing the fluid-like properties of CLC's for beam apodization of slab-geometry amplifiers or diode lasers, and also for beam apodization of rod amplifiers with large clear apertures. We will briefly review the optical properties of CLC's and then explore the design concepts of two beam apodizers based on a gradient-index optical effect in these fluids.

Optical Properties of Cholesteric Liquid Crystals

CLC's have a helical layered organization as shown in Fig. 41.20. Normally, a CLC cell is prepared between two glass substrates. Within each single layer of the structure, molecules align in a parallel configuration like nematics. The average orientation of the elongated liquid-crystal molecules is defined as the director. In adjacent layers, protruding side groups of atoms attached to each molecule force the director to be twisted. The rotation of layers through the fluid gives rise to a helical structure. One full 360° rotation of the director is defined as one pitch length P_o. This helical structure leads to the important optical property of selective reflection in circular polarization and wavelength.[13]

Our CLC's are a blend of a nematic liquid crystal and a chiral additive. The selective-reflection peak wavelength can be tuned by changing the blending ratio (or relative concentration) of these materials. In blending, adding more nematic liquid crystal increases the pitch length P_o and adding more chiral additive decreases P_o.

In Fig. 41.20 we consider a right-handed CLC cell whose helical axis is oriented along the z-axis. No interaction occurs between the right-handed helical structure of the CLC and left-handed circularly polarized light propagating through it. However, when right-handed circularly polarized light with wavelength λ propagates along the z-axis at normal incidence, the reflectivity R is given by[14]

$$R = \frac{\sin^2\left[\kappa\, L\sqrt{1-(\delta/\kappa)^2}\,\right]}{\cosh^2\left[\kappa\, L\sqrt{1-(\delta/\kappa)^2}\,\right]-(\delta/\kappa)^2}, \tag{2}$$

where $\kappa = \kappa_o \cdot (\lambda_o/\lambda)$ and $\kappa_o = (\pi/\lambda_o) \cdot \Delta n$ is the coupling coefficient; $\delta = 2\pi\,(1/\lambda - 1/\lambda_o)n_{av}$ is the detuning parameter; $\lambda_o = n_{av} \cdot P_o$ is the peak wavelength of the selective reflection band; and L is the CLC fluid thickness.
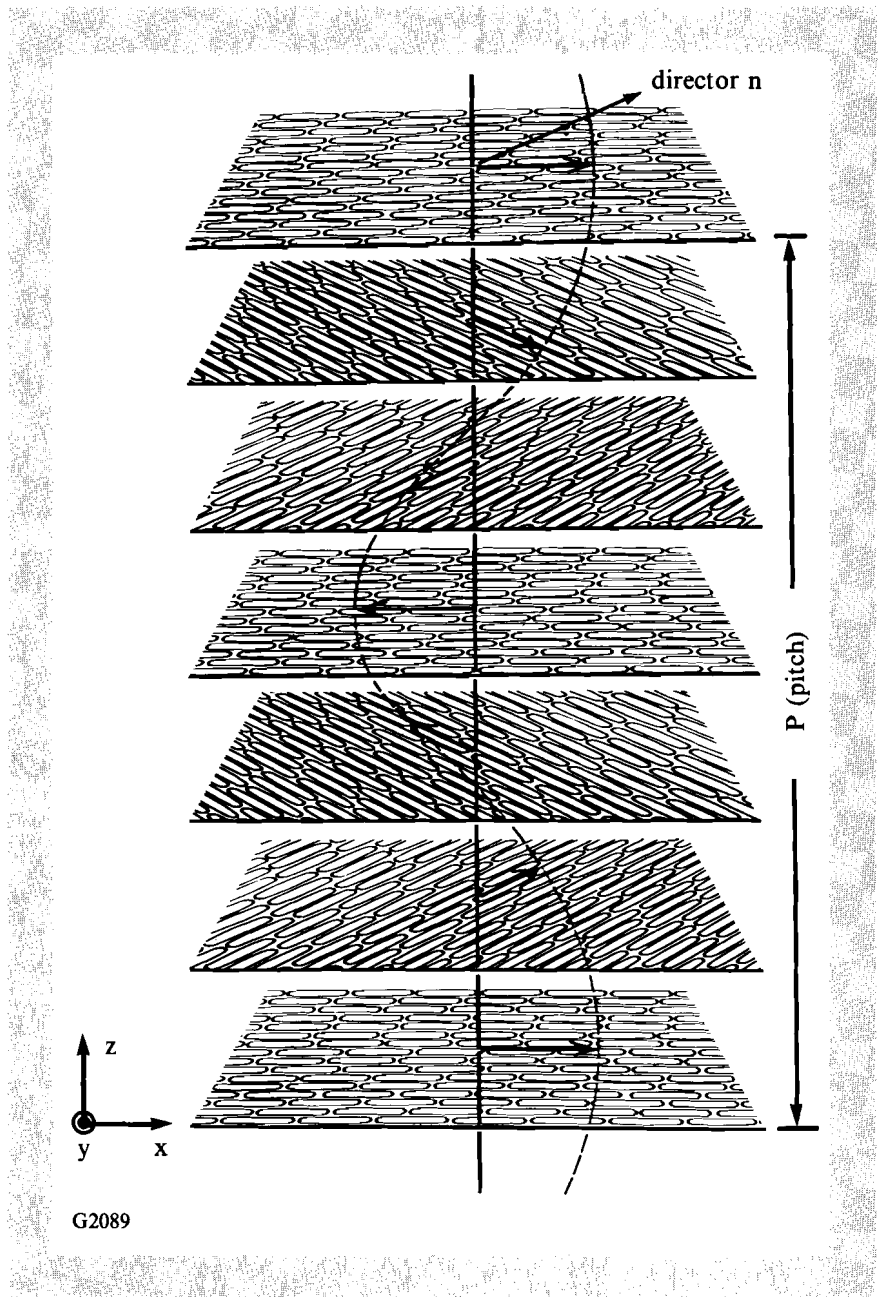
Fig. 41.20
Schematic diagram of molecular order in a cholesteric liquid crystal.

Here, Δn and n_{av} represent the optical birefringence and average refractive index, respectively. When $\lambda = \lambda_o$, the CLC structure is well phase matched to the input wavelength, and the reflectivity is equal to

$$R = \tanh^2(\kappa_o L). \tag{3}$$

A wedged cell was fabricated to confirm the relationship in Eq. (3) using the blend of a nematic liquid crystal E7 and chiral additive CB15 tuned to

31

exhibit a selective reflection peak at λ = 1064 nm. (The liquid-crystal compounds for this work were purchased from EM Chemicals, Hawthorne, NY, and used as received.) For the CLC fluid prepared, $n_{o,n} = 1.4172, n_{e,n} = 1.6014, \Delta n = 0.1842,$ and $n_{av} = 1.5093$ as determined with an Abbé refractometer (22°C, λ = 1053 nm). At λ = 1064 nm, the coupling coefficient is calculated to be $\kappa_o \cong 0.5480$. For this CLC blend, the reflectivity as a function of thickness is shown in Fig. 41.21. The close match of theoretical and experimental data supports the validity of Eq. (3).

A plot of the reflectivity R as a function of λ/λ_o for $\kappa L = 4.59$ is shown in Fig. 41.22. It can be seen that when $\lambda/\lambda_o = 1.076$, the reflectivity of the CLC goes to zero. The ripples in Fig. 41.22 are due to phase mismatching. This effect is not seen in practice for cells assembled with weak surface
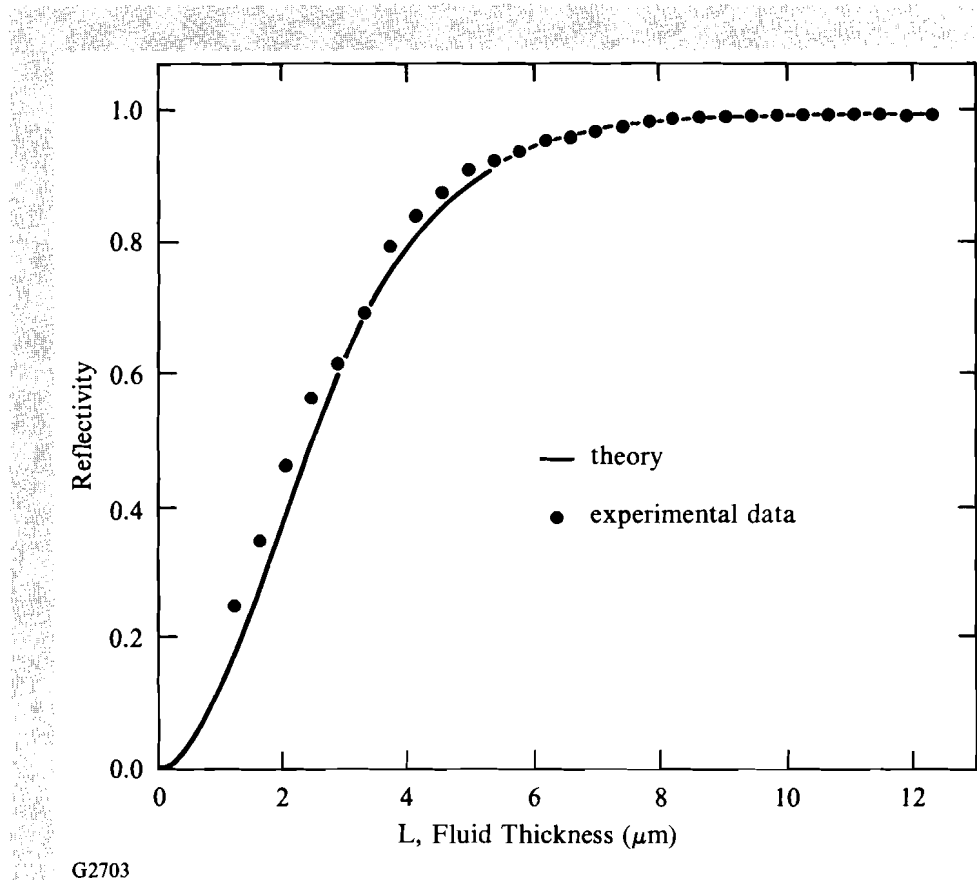

G2703

Fig. 41.21
Reflectivity R measured at λ = 1064 nm, as a function of thickness L, for a mixture of E7 and CB15 tuned to exhibit a selective peak at λ_o = 1064 nm. The coupling coefficient κ_o is 0.5439. The solid line represents the result of theoretical calculation, and the circles represent experimental data.

anchoring due to the presence of small nonuniformities through the bulk of the fluid. This weak surface anchoring (at one or both of the inner surfaces of the cell) is very important for the apodizer application described here because it prevents any discontinuity in structure[15] and concomitant deviations from a smooth reflectivity profile.

A spatial gradient in selective-reflection peak wavelength can be induced by filling a device with mixtures of two CLC fluids having different selective-reflection bands, from opposite sides of a cell as shown in Fig.
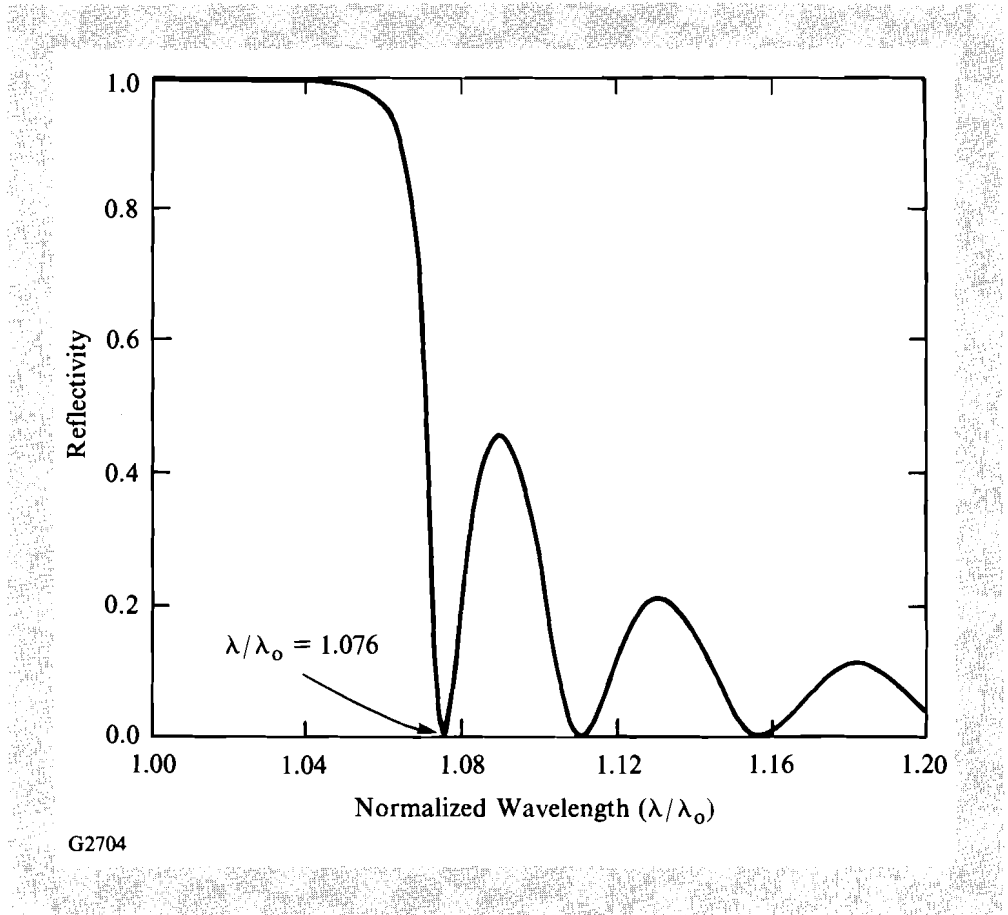
Fig. 41.22
Reflectivity R as a function of normalized wavelength λ/λ_0 for $\kappa L = 4.59$.

41.23. The fluid-like property of liquid crystals allows them to blend together in region 3. This concept will be referred to as a gradient CLC (GCLC). The blending ratio (relative concentration) of chiral additives in the nematic liquid-crystal host varies linearly in region 3 from the region-1 side to the region-2 side. Since the helix wave number of the CLC, $q_0 = 2\pi/P_0$, is proportional to the concentration,[16] δ/κ in Eq. (2) can be rewritten as

$$\frac{\delta}{\kappa}(x) = \frac{2n_{av}}{\Delta n}\left[1 - \frac{q_0(x)}{k_0}\right] = \frac{2n_{av}}{\Delta n}\left(1 - \frac{\lambda_o}{\lambda}\right), \qquad (4)$$

where $k_0 = (2\pi/\lambda) \cdot n_{av}$ is the wave number in the liquid-crystal medium. For simplicity, the average refractive index and birefringence are assumed to be constant in the wavelength regions of interest. Then λ/λ_0 changes linearly as a function of position. If two CLC's are chosen such that CLC2 has a normalized wavelength λ/λ_0 that gives rise to high reflectivity and CLC1 has $\lambda/\lambda_0 = 1.076$, a smooth-edge profile can be created in the overlap region as shown in Fig. 41.23. Assuming that the width of the overlap region is held constant, the slope of the transmission function across the overlap region can be varied by tuning the λ/λ_0 of CLC2 used for high reflection in region 2 of Fig. 41.23. As the λ/λ_0 in region 2 approaches 1.076, the slope across the

33

region 3 (gradient pitch from P_1 to P_2)

region 1
(pitch P_1)

region 2
(pitch P_2)

fill direction
CLC1

fill direction
CLC2

CLC1: high transmission at a
design wavelength

CLC2: high reflection at a
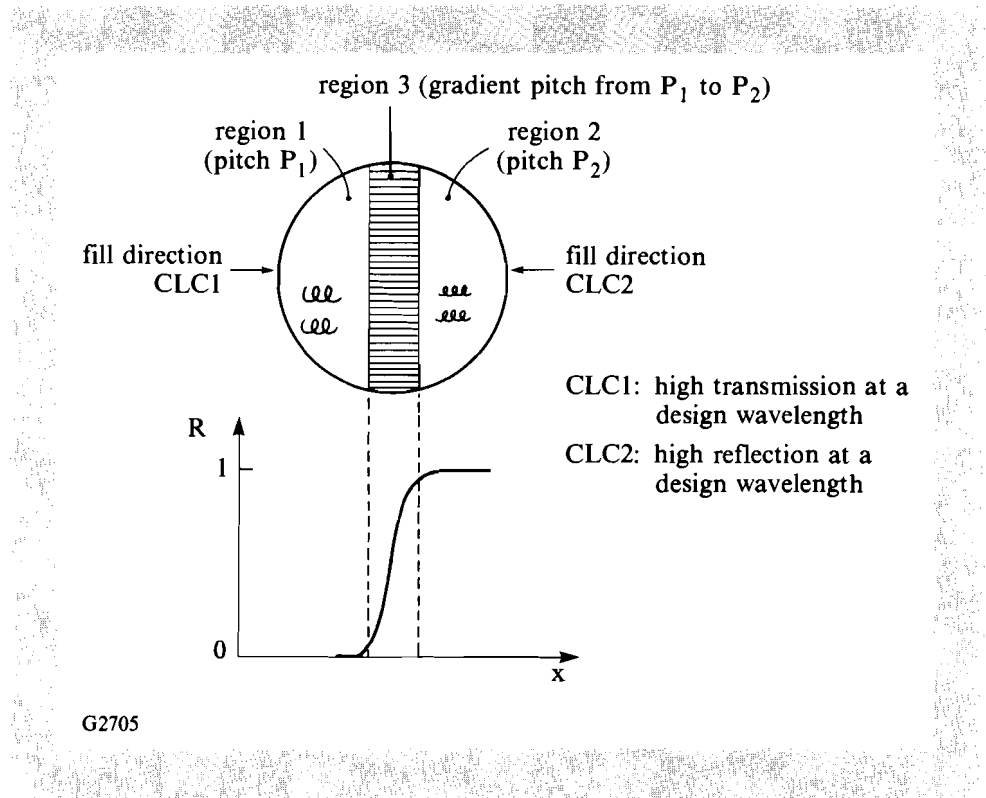design wavelength

R

1

0

x

G2705

Fig. 41.23
Reflectivity profile for a gradient cholesteric liquid-crystal element. The fluid-like
property of cholesteric liquid crystals allows them to mix over a finite region of
contact and create a pitch gradient. This results in a smoothly varying reflectivity
profile.

overlap region (region 3) is reduced, resulting in a softer reflectivity edge
profile for the device.

There are several ways to create shaped gradients in Δn and n_{av}: (1) by
using the same host nematic with different concentrations of the same chiral
additive resulting in two distinctly different selective-reflection bands with
similar Δn; (2) by using different host nematics (allowing for variability in
viscosity and birefringence) with the same chiral additive; and (3) by using
different host nematics with different chiral additives.

Implementation of Beam Apodizers
1. One-dimensional apodizer

Three cleaned, uncoated, nearly identical 38-mm-diameter GCLC cells
were assembled from borosilicate glass (BK-7) substrates. For each cell, the
gap thickness was set at 13 μm with Mylar® spacers. Filling was done by
capillary action at 60°C, above the isotropic transition temperature of
nematic E7, with two different right-handed CLC blends, each containing a
different amount of the chiral additive CB15. One CLC was tuned to exhibit
a selective-reflection peak at $\lambda_o = 1064$ nm at 22°C, the other at $\lambda_o = 820$ nm.
A near-planar structure was produced by the usual method of shearing.
Figure 41.24 gives reflection spectra in the form of optical density for each

CLC mixture in the visible and near infrared at 22°C. These spectral scans were taken with unpolarized optical radiation in a spectrophotometer (Perkin-Elmer Lambda-9). As mentioned earlier, the side lobes (or ripples) do not appear in spectra under conditions of weak anchoring, due to the nonuniformities in helix wave number of the molecules in the bulk. The slight tilt of the flat-top region and the asymmetric selective-reflection peak shapes in these scans come from a slight tilt in the planar structure induced by inner-substrate surface effects. The degree of selective reflection, as indicated by the magnitude of the change in optical density, ΔO.D., from the base line, is equal to about 0.29, which shows good alignment. (The theoretical limiting value is equal to log 2 = 0.3.)
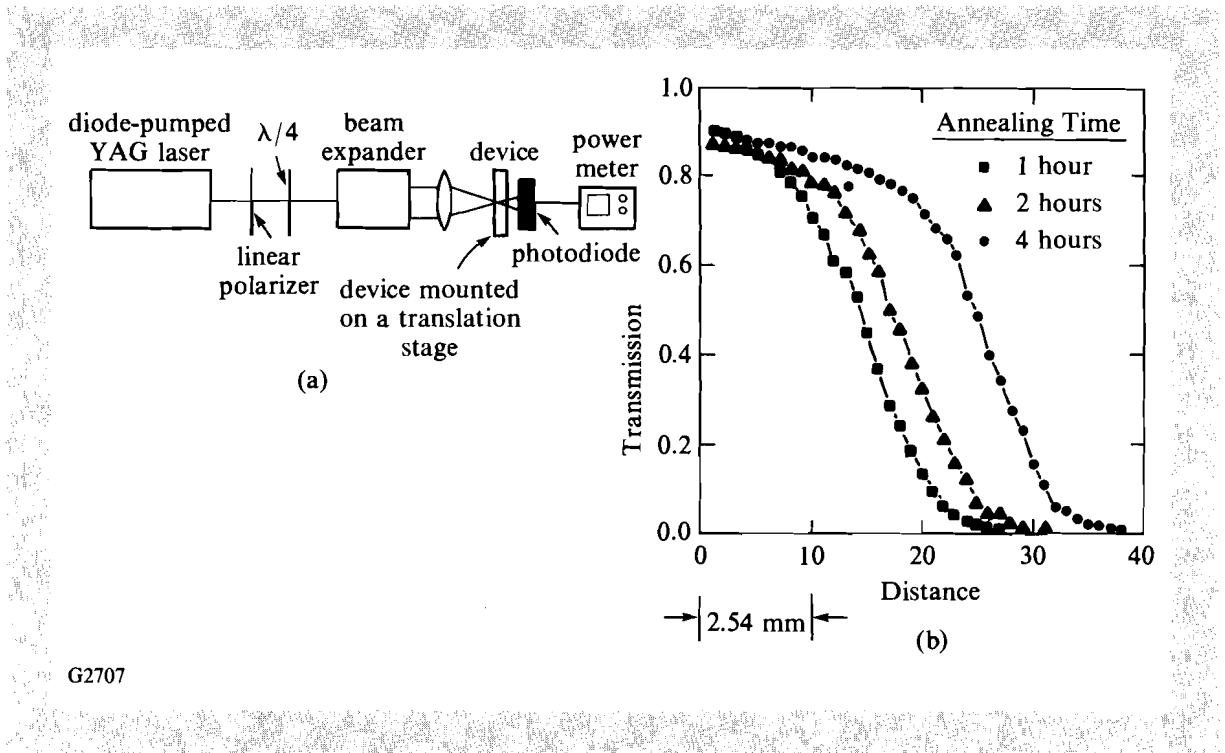
The experimental setup used to measure apodizer transmission profiles is shown in Fig. 41.25(a). The output of a diode-pumped Nd:YAG laser (Amoco Micro Laser at 1064 nm) is converted to right-handed circularly polarized light, collimated and focused onto a GCLC cell (500-μm spot size).
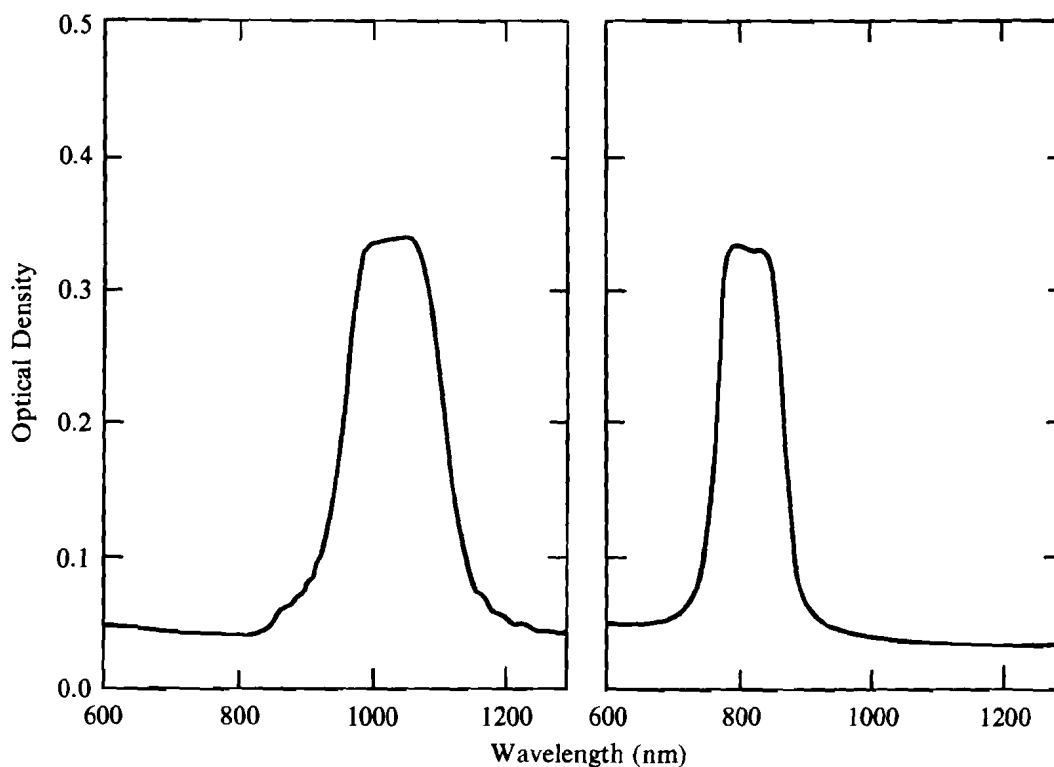
G2706

Fig. 41.24
Individual selective-reflection bands for two different cholesteric liquid crystals used in fabricating a GCLC element.

The cell is scanned by passing through the beam on a translation stage. Transmitted light intensity is measured using a photodiode detector (United Detector Technologies, UDT-10). Figure 41.25(b) shows the transmission profiles of the three GCLC cells taken at T = 22°C. The size of the interface region is determined and can be controlled by the length of time during which the filled device is annealed at a temperature above the isotropic phase-

Fig. 41.25
(a) Experimental apparatus used to measure transmission profiles of apodizers.
(b) Transmission profiles for three gradient GCLC's as a function of position after annealing periods of
   1 h, 2 h, and 4 h in the isotropic phase.

transition temperature of the mixtures. This keeps fluid viscosity low and permits *in situ* blending to occur.

The concept of controlled fluid blending to create a linear optical gradient can be exploited to make a one-dimensional rectangular beam apodizer as shown in Fig. 41.26. This device can be constructed by taking two nearly identical GCLC cells whose fabrication was described above, and overlaying them as shown in the figure. In this configuration, the light is transmitted only in the overlap region where transmission (*T*) occurs for both cells. In the *R* regions light will be blocked by selective reflection. A transmission profile across one such apodizer is shown in Fig. 41.27. The clear aperture of the device can be adjusted by mechanically sliding the two GCLC elements relative to each other.

2. Circular beam apodizers of large clear aperture

Geometrical constraints to liquid-crystal apodizer construction using previous designs[12] makes scaling up to apertures greater than 6 mm difficult. These difficulties are eliminated by designing an apodizer that consists of a single, homogeneous CLC fluid between a plano-convex lens with radius of curvature ρ and a plano-concave lens with radius of curvature ρ', the curved surfaces forming the inner wall. The two substrates have slightly different inner radii of curvature. Index matching between fluid and substrate lens
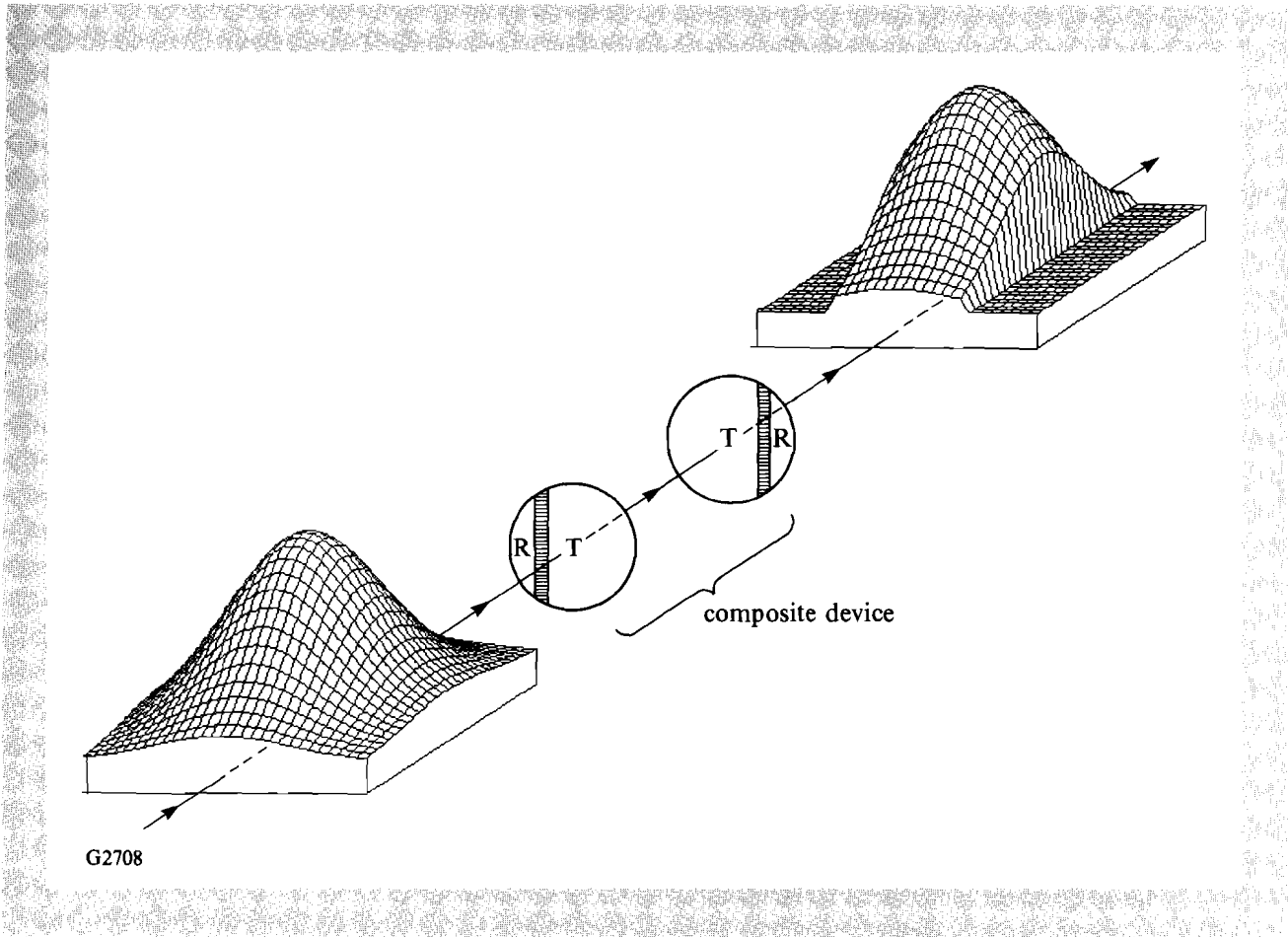
G2708

Fig. 41.26
A one-dimensional beam apodizer can be obtained by stacking a pair of two complimentary CLC cells. A variation in lateral position of the cells relative to each other allows for the adjustment of the clear aperture. In this illustration, R represents reflection of the incident beam, T represents transmission. The shaded area represents the mixing region in each element where a pitch gradient exists.

elements is important to remove focusing. This requires that the average refractive index of the substrates should be close to n_{av} of the fluid. The gap thickness between the two substrates is given by

$$L(r) = \frac{r^2}{2\rho}\left[1 - \frac{\rho}{\rho'}\right] \tag{5}$$

The transmission profiles for $\rho/\rho' = 0.863$ and $\rho/\rho' = 0.9$ with $\rho = 1033.4$ mm are shown in Fig. 41.28 as two solid lines. As ρ/ρ' increases, that is, as the radii of curvature for the two substrates approach each other, the clear aperture of the apodizer increases. In this figure, the dotted lines represent
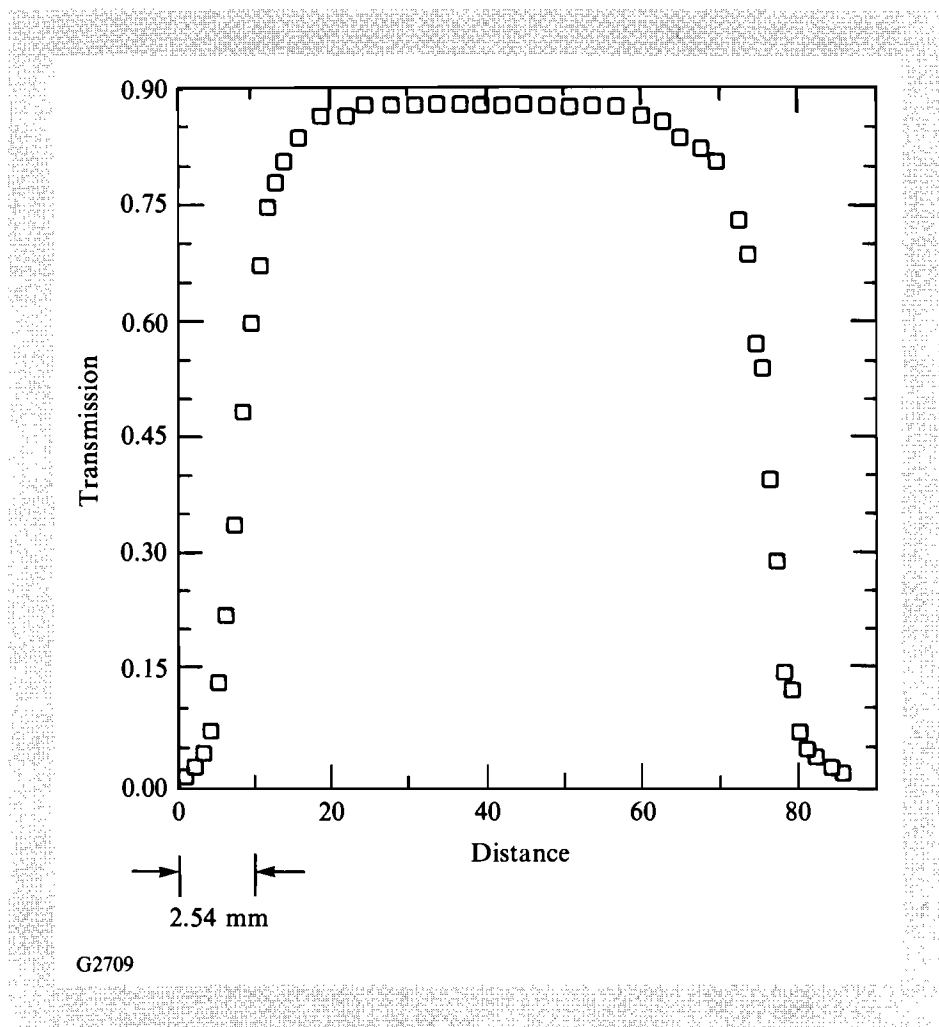
Fig. 41.27
Transmission profile of a one-dimensional apodizer. GCLC's that were annealed in the isotropic phase for 1 h and 2 h were chosen to construct the composite device.

a super-Gaussian fit to the transmission profiles. Both fits show that the order of the super-Gaussian is $N = 3.51$. As long as the CLC fluid thickness is varied according to Eq. (5), the order of the apodizer is invariant and equal to $N = 3.51$ for this design.

Two 50.8-mm-diameter substrates with $\rho = 1033.4$ mm and $\rho' = 1197.5$ mm were obtained and assembled into a cell. The air gap was filled by capillary action at 60°C with a homogeneous mixture of E7 and CB15 tuned to 1064 nm as shown in Fig. 41.29. The measured (circles) transmission for the device at 22°C and calculated (solid line) profiles as a function of radius are shown in Fig. 41.30. Super-Gaussian fits to both curves (dashed lines) give $N = 3.51$ ($r_o = 8.5$ mm) for the theoretical data and $N = 3.52$ ($r_o = 9.9$ mm) for the experimental data. Local misalignment of molecules in the CLC can cause the coupling coefficient to be lower than the theoretical value, explaining the discrepancy. In general, a super-Gaussian apodizer of order greater than 3.51 is required in high-power laser applications to maximize output energy.[1] This cannot be achieved with the simple, single-fluid concept demonstrated above, because the order N of the super-Gaussian cannot be varied. The addition of a gradient-index effect, however, permits orders greater than 3.51 to be constructed.
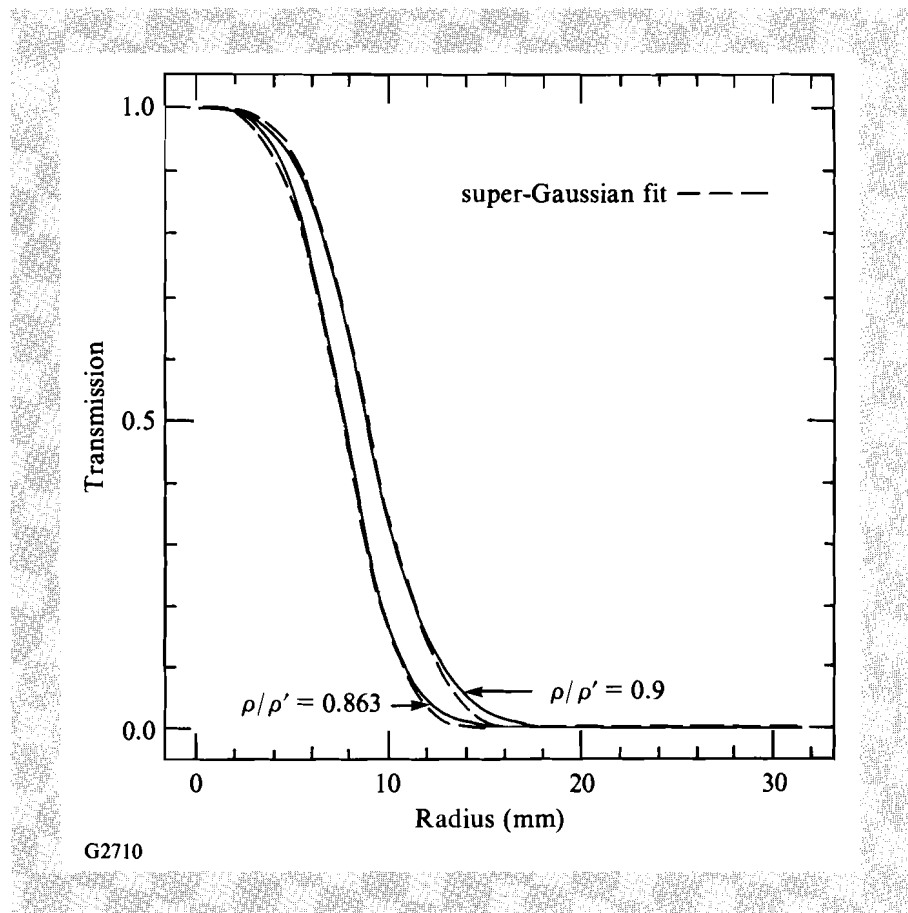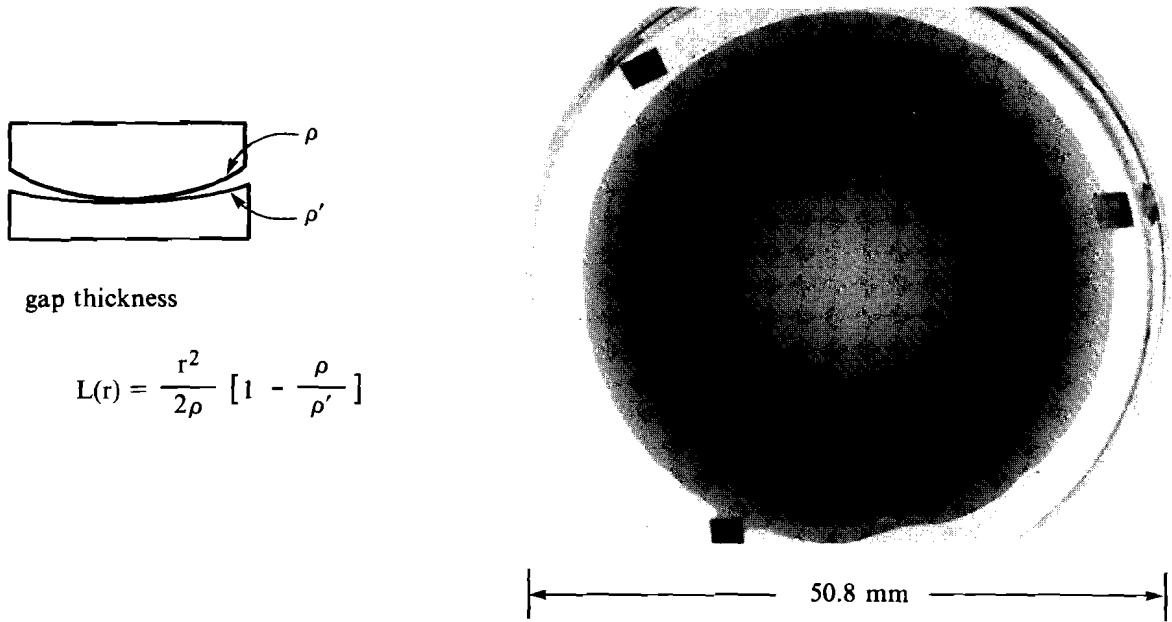
Fig. 41.28
Calculated edge-transmission profiles for two CLC beam apodizers with $\rho/\rho' = 0.863$ and $\rho/\rho' = 0.9$ (two solid lines). Here dotted lines represent super-Gaussian fits for each case.

3. Gradient-index circular apodizers

The GCLC concept can be used to construct circular apodizers with a wider range of profiles. The concept is shown in Fig. 41.31. In this figure, CLC1 has high transmission and CLC2 has high reflection at the design wavelength. The fluid-like properties of CLC's allow them to mix together and form a pitch-gradient region where the reflectivity changes from 0 to 1 outward radially from the center of the device. Good circular symmetry can be achieved by using slightly different radii of curvature for the supporting substrates so that CLC1 is drawn into the narrow gap area in the center by radial capillary action.

In order to prove the concept, two 50.8-mm-diameter substrates with $\rho = 1033.4$ mm and $\rho' = 1197.5$ mm were chosen to assemble a cell. Mixtures of ZLI1167 and CB15 (isotropic at 90°C, tuned to 910 nm) and E7 and CB15 (isotropic at 60°C, tuned to 1064 nm) were used as CLC1 and CLC2, respectively. This device is designed such that, with curved surfaces acting as the inner cell walls, the gap thickness at the inner edge of the CLC2 band is sufficient to give high reflection.

Fabrication required several steps. First, CLC1 was filled by capillary action at 90°C until it assumed a good circular symmetry at the center of the cell. The cell was then cooled to 45°C and CLC2 was loaded in very slowly, so as not to initiate mixing. CLC1 tended to resist deformation because of

gap thickness

$$L(r) = \frac{r^2}{2\rho} \left[1 - \frac{\rho}{\rho'} \right]$$

G2711

Fig. 41.29
Photograph, between linear polarizers, of a 1064-nm CLC circular beam apodizer made from off-the-shelf plano-concave/convex lenses ($\rho = 1033.4$ and $\rho' = 1197.5$). The schematic diagram indicates the assembly orientation and the resulting relationship for fluid gap L, as a function of radial dimension r.

its increased viscosity at the lower temperature. Once the filling of CLC2 was done, the temperature was increased to 90°C for a 1-h anneal in the isotropic phase of both blends. The element was then cooled to room temperature and sheared to get good alignment.

Experimental data (circles) taken at 22°C and a super-Gaussian fit (dashed line) are shown in Fig. 41.32. This apodizer profile is seen to match a super-Gaussian of order $N = 8.3$ with $r_o = 12.4$ mm. The deviation from ideal performance in the central flat-top region, where high transmittance is required, is a result of residual reflectance at 1064 nm from the wing of the CLC1 reflection band centered at 910 nm. It can be eliminated by preparing a CLC1 blend that has a selective-reflection peak at a shorter wavelength than 910 nm. The slope at the edge of the apodizer can be changed by varying the length of time at which the filled device is thermally annealed at a constant temperature above the isotropic phase-transition temperatures of the mixtures, where the viscosities are low. A slight asymmetry to the apodizer profile seen in Fig. 41.32 is the result of a wedge inadvertently introduced by epoxy in a sealing operation.

Fig. 41.30

Transmission profile at λ = 1064 nm, for a circular CLC apodizer filled with a homogeneous fluid (mixture of E7 and CB15). The solid line is the calculated transmission profile for an ideal case, the circles are the experimental results and the dotted lines represent the best super-Gaussian fit to the data (N = 3.51).
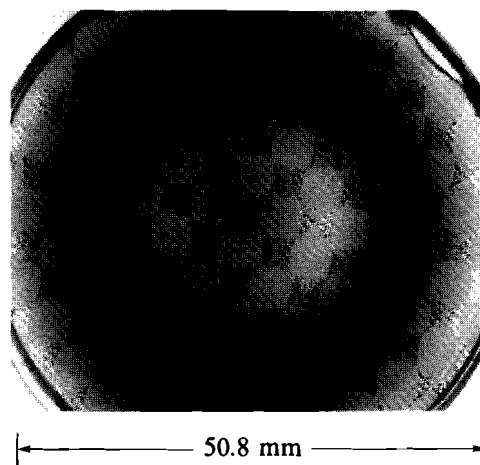
G2712

G2713

50.8 mm
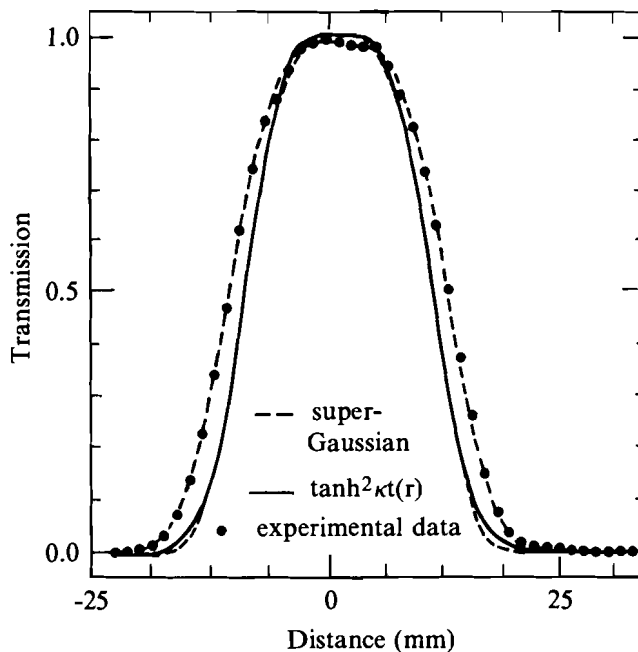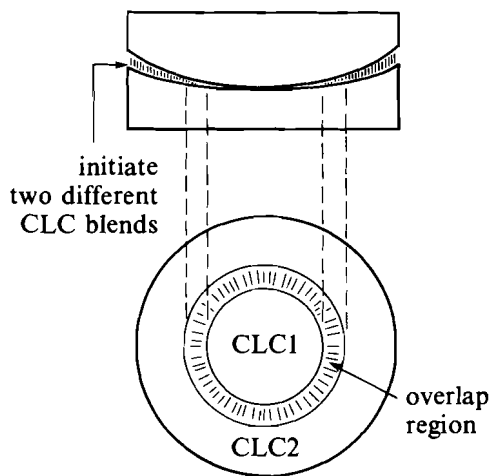
Fig. 41.31

Photograph, between two linear polarizers, of a 1064-nm GCLC beam apodizer. For this apodizer, the mixture of CB15 in ZLI1167, tuned to 910 nm is used as CLC1; the mixture of CB15 in E7, tuned to 1064 nm is used as CLC2.
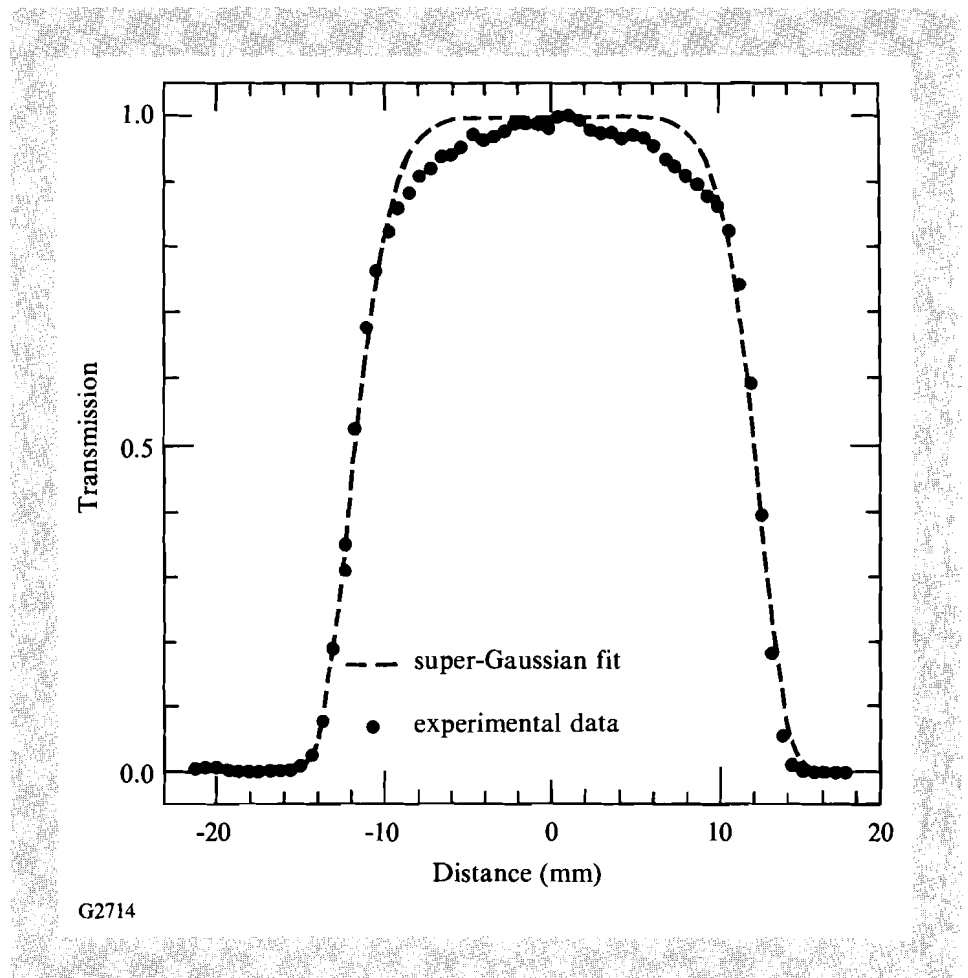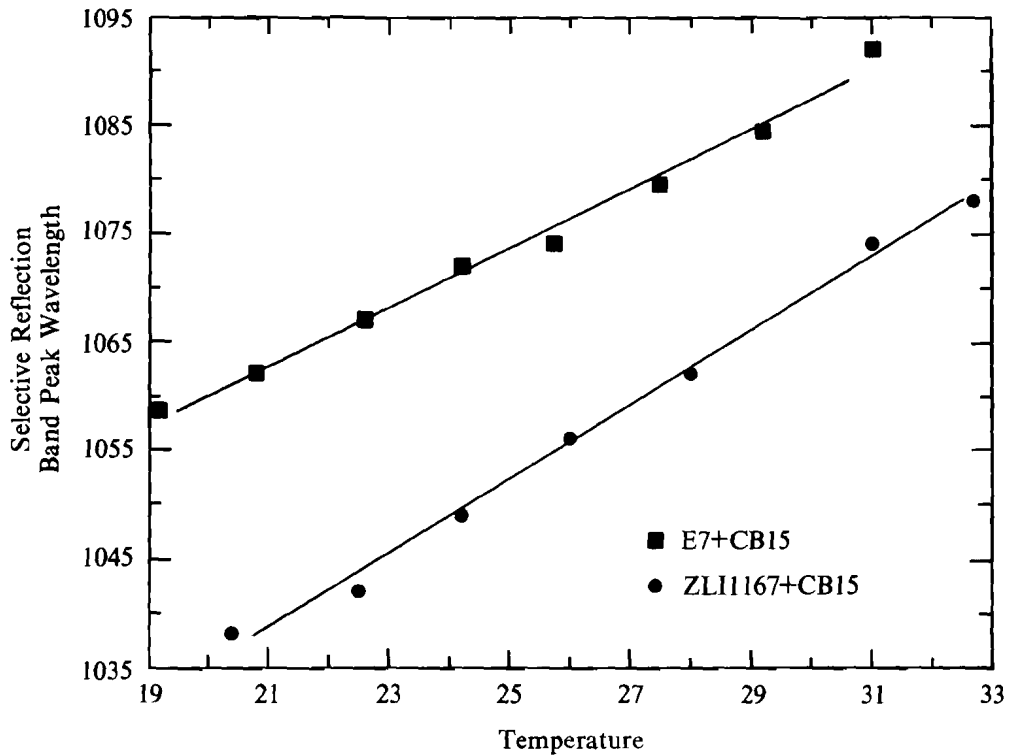
Fig. 41.32
Transmission profile of the GCLC apodizer in Fig. 41.31 at $\lambda = 1064$ nm. The circles are the experimental results and the dotted line represents the best super-Gaussian fit to the data ($N = 8.3$, $r_0 = 12.4$ mm).

Temperature changes can cause wavelength shifts to the features of liquid-crystal devices. Temperature dependence of the selective-reflection peak wavelengths for the two CLC's used to make the graded-index circular apodizer are shown in Fig. 41.33. In the temperature range of 20°C to 30°C, the selective-reflection peak wavelength is shifted 2.8 nm /°C for the mixture of E7 and CB15 and 2 nm /°C for the mixture of ZLI1167 and CB15. New chiral dopants have recently been described that could be employed to reduce temperature sensitivity of CLC mixtures.[17]

The laser-damage thresholds for GCLC apodizers depend largely upon the compounds used for blending. Since 1986 CLC devices up to 100 mm in diameter have been used as circular polarizers in more than 60 positions on OMEGA.[12] Extensive system testing of assembled polarizer elements and off-line laser-damage experiments on the fluids themselves have found that blends like CB15 in E7 have intrinsic laser-damage thresholds of about 5 J/cm² (1-on-1 or n-on-1 at 1054-nm, 1-ns, 3-mm spot). Fluid blends that

Fig. 41.33
Change in selective-reflection peak wavelength as a function of temperature for the
ZLI1167 + CB15 (circles) and the E7 + CB15 mixtures (squares).

contain base nematics like ZLI1167 have recently been shown to be at least
three times more resistant to bulk laser damage under identical conditions,
because of their more nearly saturated chemical structure.[18] Wave-front
quality has not yet been measured for these apodizers, but it should be better
than λ/4 based on our previous work.[12]

Summary

We have described the design, fabrication, and characterization of laser-
beam apodizers based upon gradient-index optical effects in liquid crystals.
For a one-dimensional apodizer design, the clear aperture was shown to be
variable by means of sliding two device elements over each other. The order
of the super-Gaussian edge profile was maintained. A circular apodizer, in
which the thickness variation of CLC fluid was defined by two substrates
with different inner-surface radii of curvature, had a fixed-edge profile given
by a super-Gaussian order of $N = 3.51$. The ability to vary N in this design
was established by using the mixing property of liquid crystals to create a
gradient-index optical effect. For this application it is important to have
weak anchoring only, at either one or both of the inner surfaces of the
apodizer, to prevent any discontinuity in structure.

ACKNOWLEDGMENT

REFERENCES

1. V. R. Costich and B. C. Johnson, *Laser Focus* **10**, 43 (1974).

2. A. Penzkofer and W. Frohlich, *Opt. Commun.* **28**, 197 (1979).

3. Y. Asahara and T. Izumitani, U.S. Patent 4,108,621 (August 22, 1978).

4. G. Dubé, *Advanced Laser Technology and Applications*, edited by L. Esterowitz, *Proc. Soc. Photo-Opt. Instrum. Eng.* **335**, 10 (1982).

5. V. I. Kryzhanovskii *et al., Sov. J. Quantum Electron.* **13**, 194 (1983).

6. A. J. Campillo, B. Carpenter, B. E. Newnam, and S. L. Shapiro, *Opt. Commun.* **10**, 313 (1974).

7. E. W. S. Hee, *Opt. Laser Technol.* **7**, 75 (1975).

8. S. B. Arifzhanov *et al., Sov. J. Quantum Electron.* **11**, 745 (1981).

9. G. Dubé, *Opt. Commun.* **12**, 344 (1974).

10. J.-C. Diels, *Appl. Opt.* **14**, 2810 (1975).

11. B. J. Feldman and S. J. Gitomer, *Appl. Opt.* **16**, 1484 (1977).

12. S. D. Jacobs, K. A. Cerqua, K. L. Marshall, A. Schmid, M. J. Guardalben, and K. J. Skerrett, *J. Opt. Soc. Am. B* **5**, 1962 (1988).

13. J. L. Fergason, *Liquid Crystals: Proceedings of the International Conference on Liquid Crystals*, Kent State University, 16–20 August 1965, edited by G. H. Brown, G. J. Dienes, and M. M. Labes (Gordon and Breach, New York, 1967), p. 89.

14. J. C. Lee, J. H. Kelly, D. L. Smith, and S. D. Jacobs, *IEEE J. Quantum Electron.* **24**, 2238 (1988).

15. P. D. de Gennes, *The Physics of Liquid Crystals* (Oxford, Claredon, 1974), p. 264.

16. *Ibid*, p. 240.

17. F. Leenhouts, S. Kelly, and A. Villiger, *Appl. Phys. Lett.* **54**, 696 (1989).

18. M. Guardalben, A. Schmid, S. D. Jacobs, and S. H. Chen, presented at the First International Symposium on Nonlinear Optical Polymers, Natick, MA, 13–14 June 1988. See also: M. Guardalben, A. Bevin, K. Marshall, and A. Schmid, *Proceedings, 20th Annual Symposium on Optical Materials*, Boulder, CO, 26 October 1988, in press.